Liquid Crystals
Publication details, including instructions for authors and subscription information:
http://www.informaworld.com/smpp/title~content=t713926090

Determination of the torsional anchoring of a twisted nematic liquid crystal using the half-leaky guided mode technique

F. Z. Yang[a]; H. F. Cheng[a]; H. J. Gao[a]; J. R. Sambles[b]
[a] Liquid Crystal Research Center, Department of Chemistry, Tsinghua University, Beijing 100084, PR China, [b] Thin Film Photonics, School of Physics, University of Exeter, Stocker Road, Exeter EX4 4QL, UK,

Online publication date: 06 August 2010

To cite this Article Yang, F. Z. , Cheng, H. F. , Gao, H. J. and Sambles, J. R.(2001) 'Determination of the torsional anchoring of a twisted nematic liquid crystal using the half-leaky guided mode technique', Liquid Crystals, 28: 1, 51 — 57
To link to this Article: DOI: 10.1080/026782901462373
URL: http://dx.doi.org/10.1080/026782901462373

LIQUID CRYSTALS, 2001, VOL. 28, NO. 1, 51–57

Determination of the torsional anchoring of a twisted nematic liquid crystal using the half-leaky guided mode technique

F. Z. YANG, H. F. CHENG, H. J. GAO

Liquid Crystal Research Center, Department of Chemistry, Tsinghua University, Beijing 100084, PR China

and J. R. SAMBLES*

Thin Film Photonics, School of Physics, University of Exeter, Stocker Road, Exeter EX4 4QL, UK

(*Received 14 April 2000; in final form 5 June 2000; accepted 4 July 2000*)

Optical excitation of half-leaky guided modes has been used to explore the director profile of a thin twisted homogeneously aligned nematic liquid crystal cell (Merck, E7). Twisted alignment is realized by the use of rubbed polyimide layers on both inner walls of the cell. By modelling the optical response of particular director profiles in the cell to fit the half-leaky guided mode reflectivity data, both the thickness and the twist of the director from the top to the bottom of the cell are accurately determined. Then comparing the rubbing directions with the twist of the easy axes, the torsional anchoring coefficient, W_T is quantified through a knowledge of the twist elastic constant K_{22} of E7. At 24.5°C we find that $W_T = (5.8 \pm 0.4) \times 10^{-5}$ J m^{-2}.

1. Introduction

The surface alignment of nematic liquid crystals (NLCs) on specially treated substrates is very important for the repeatable fabrication of test cells for fundamental science research, as well as for the production of devices. It is a subject that, because of the wide application of liquid crystal displays (LCDs), has received considerable attention. A number of techniques for creating good quality surface alignment have been developed and the characteristics of the surface anchoring explored. Because the response of a LCD to driving voltages is strongly influenced by surface anchoring, then for the design of cells it is important to have accurate determination of this surface anchoring.

The surface alignment of LCs can be characterized in terms of a polar anchoring energy, constraining the out-of-plane motion of the director and a torsional or azimuthal anchoring energy restricting the in-plane motion of the director. It is these energies that determine to what extent an alignment surfactant will hold a liquid crystal director in a desired orientation and thus how well suited it is to a particular task. The polar anchoring energy can be measured by the application of fields that cause director lift-off at the surface [1–3]. However the torsional anchoring energy is generally determined by either an external field technique [4–7] or by some geometrical procedure [8–11] involving the measurement of the surface twist-off for a twisted nematic cell (TN cell). In the external field technique an electric or magnetic field is applied to distort the bulk director in the cell, this distortion being balanced by elastic forces that are constrained by the boundary anchoring. In principle, by varying the external field, both the twist elastic constant, K_{22}, and the surface torsional anchoring coefficient, W_T, can be deduced. However the mathematics and the experimental procedure of this technique are complex, leading to difficulties in obtaining reliable data. In the second technique that involves the measurement of a twisted nematic liquid crystal cell with known surface alignment directions, the twist-off of the director at the surface is brought about by an equilibrium between the two surface torsional terms balanced by a bulk elastic twist. Measuring the surface twist-offs from the original alignment axes will then lead to a knowledge of the ratio W_T/K_{22}. It is clear that in order to quantify W_T the twist elastic constant K_{22} has to be determined separately. However because no external field is needed to distort the director profile in the cell and since K_{22} may be readily found in data from chemical suppliers, this second technique for quantifying W_T is widely used.

The key point in quantifying the torsional anchoring strength using the twist-off technique is the accurate determination of the total twist angle of the liquid crystal

*Author for correspondence; e-mail: J.R.Sambles@exeter.ac.uk

Liquid Crystals ISSN 0267-8292 print/ISSN 1366-5855 online © 2001 Taylor & Francis Ltd
http://www.tandf.co.uk/journals

director, ϕ_t, which is compared with the externally imposed alignment twist, ϕ_t^0, that is, the angle between the two 'easy' axes on the two surfaces of the cell. The difference between the two angles is the sum of the twist-offs at both boundaries. Based upon a Jones matrix optical analysis and normal-incident transmissivity measurements, several experimental procedures [8–11] have been developed to determine ϕ_t, and hence, through a knowledge of ϕ_t^0, the torsional anchoring strength. However, optically a liquid crystal cell may not be treated in the same manner as a slab of uniaxial material. The liquid crystal is always surrounded by partially reflecting layers, the reflections from which are ignored in the Jones matrix approach taken by various workers. In our recent work [12], we have examined a liquid crystal cell as an optical multi-layer system and used Berreman's 4×4 matrix approach to model the normal-incident transmission. The results show clearly that the Jones' 2×2 matrix approach is likely to give wrong values for the strength of torsional anchoring at the surface of the cell. So an optical method based on the correct determination of the real director twist angle in a twisted nematic cell is needed.

In this present study, our recently developed optical procedure—the half-leaky guided mode (HLGM) technique [13, 14]—has been used to excite a series of half-leaky guided modes in a thin twisted nematic liquid crystal cell (Merck E7). Homogeneous, twisted, alignment is realized by rubbed polyimide coatings on the inner walls of the cell. The reflectivity data from the half-leaky guided modes are very sensitive to the director profile of the liquid crystal in the cell. By using multi-layer optics theory to predict the optical response of a range of model director profiles, and thereby to fit the reflectivity data of the half-leaky guided modes, the thickness and the twist of the director from the top to the bottom of the cell are accurately determined. By comparing this with the twist of the easy axes, that is the rubbing directions on the two surfaces, the torsional anchoring strength W_T is quantified through knowledge of the twist elastic constant K_{22} of E7.

2. Numerical modelling

Reflectivity spectra of half-leaky guided modes are dependent on the optical properties of the whole liquid crystal cell [13, 14], including the optical parameters of every layer. The primary task of this study is to determine accurately the twist profile of the director in the TN cell. To do this we first numerically compute the reflectivity spectra of a model cell which closely mimics the real cell to be studied, to find the best incidence angle and incidence plane to give the highest sensitivity to small changes of the twist-off angle of the director.

The geometrical frame of the system to be considered is illustrated in figure 1. Monochromatic plane wave radiation (He-Ne laser) is incident in the plane ZOY, with an internal incidence angle β from the Z-axis. The director of the liquid crystal, $\mathbf{n}$, has tilt angle θ from the Z-axis, and twist angle ϕ from the X-axis; in figure 1 we set $\theta_1 = \theta_2 = 90°$, $\phi_1 < 0$, $\phi_2 > 0$. The set-up comprises a high index entrance glass plate, a rubbed polyimide coating, the twisted nematic LC layer, a second rubbed polyimide coating and a low index exit glass plate. For the modelling we use the following parameters: for the high index top glass plate and optical permittivity $\varepsilon_H = 2.9998$; for the rubbed polyimide coatings, $\varepsilon_P = 2.3500 + i\,0.0020$ with thickness $d_P = 50.0$ nm; for the nematic liquid crystal layer, $\varepsilon_{\parallel} = 2.9900 + i\,0.0005$, $\varepsilon_{\perp} = 2.3000 + i\,0.0005$ with the tilt angle of the director set at $\theta = 90°$ through the cell, while the twist angle varies through the cell according to different models. Experimentally, in order to avoid the formation of two domains in the TN cell, the total angle of twist between the easy axes, ϕ_t^0, is normally set a little smaller than 90° and hence we may suppose the actual liquid crystal twist, ϕ_t is about 80° for the modelling. The thickness of the liquid crystal is $d_{LC} = 1.500\,\mu$m and for the low index bottom glass plate, $\varepsilon_L = 2.1207$. The use of a thin cell ($d_{LC} = 1.500\,\mu$m) gives a large twist-off, $\Delta\phi\,[= (\phi_t^0 - \phi_t)/2]$ ensuring more accurate determination of the surface anchoring. Because the director twist varies strongly through the cell, the p (TM) to s (TE) polarization conversion in the half-leaky guided mode spectra will be very strong. Consequently the R_{PP}, R_{SS}, R_{PS} and R_{SP} reflectivity spectra will have strong characteristic modes, as shown in figure 2(*a*) for the model $\phi_1 = -55.0°$ and $\phi_2 = 25.0°$, with a linear variation between. From figure 2(*a*) we can see that there are two special internal angles of incidence that divide the spectra into three different areas. The first is $\beta_1 = 57.23°$, which is a critical

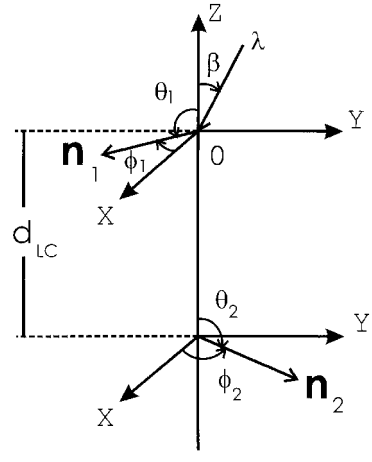

Figure 1. The frame of the TN cell for modelling.

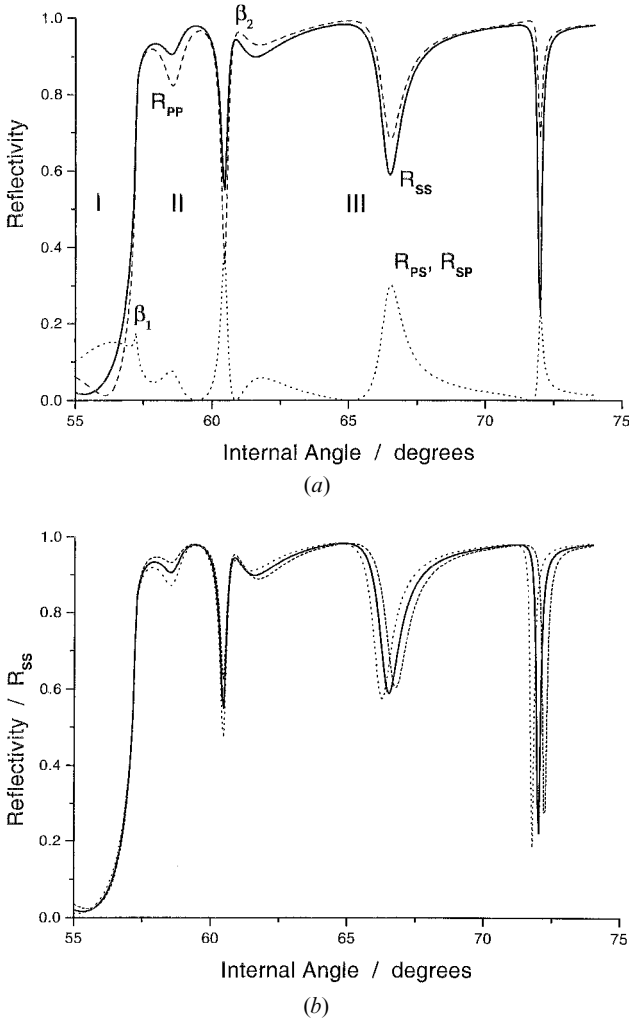

Figure 2. (*a*) Reflectivity data R_{SS}, R_{PP}, R_{PS} and R_{SP} for a given twist-off situation; (*b*) reflectivity data R_{SS} for three different twist-off situations.

angle between the high and low indices of the top and bottom glass plates. So area I is a fully-leaky guided mode area. The second angle is $\beta_2 = 60.90°$ which is very close to the pseudo-critical angle between the high index of the top glass plate and the ordinary index of the uniaxial NLC. A small difference exists between the simply calculated pseudo-critical angle and that computed using a multilayer matrix approach, because the NLC layer is not infinitely thick. Because the long axis of the index-ellipsoid, the director, of the NLC lies in the plane XOY, there is always the same pseudo-critical angle for a TM wave independent of the details of the twist angle profile. This then implies that the guided mode spectra in area II are very insensitive to the twist angle distribution through the cell. However in area III, the guided mode spectra will mainly depend upon the effective extraordinary index of the NLC, i.e. the director twist angle distribution, and so in this region the guided mode spectra will be very sensitive to the twist distribution. This means that for accurate determination of the twist-off in the TNLC cell we should work in area III. This is shown in figure 2 (*b*), in which the reflectivity, R_{SS} is modelled; the solid line is for a linear twist distribution from $-55.0°$ to $25.0°$, the dotted line is from $-57.0°$ to $27.0°$ and the dashed line is from $-53.0°$ to $23.0°$. It is very clear that even for quite big changes of the twist-off situation, the guided mode positions in area II do not change in position, only in depth. However in area III, the guided modes clearly have distinguishable movement (later, in figure 4 we shall see that we can detect twist-offs as small as 0.1°). Ideally it would appear that going to even higher angles is preferable, but experimental constraints limit the accessible internal angle to 74.0° and so the lowest order mode in area III has not been explored.

Another set of modelling is performed to find the incidence plane to obtain the best sensitivity to the director twist-off. For the same twist profile, but different starting twists, the reflectivity spectra, R_{SS}, in the area III are shown in figure 3. In figure 3 (*a*), the solid line is for a linear twist angle profile from $-40.0°$ to $40.0°$, the dotted line is for $-55.0°$ to $25.0°$, the dash-dot line is for $-75.0°$ to $5.0°$ and the dashed line is for $-90.0°$ to $-10.0°$. In figure 3 (*b*), the solid line is the same as in figure 3 (*a*) while the dotted line is for $-20.0°$ to $60.0°$ and the dashed line is for $0.0°$ to $80.0°$. From the two figures we note that on increasing the top surface director twist ϕ_1 from $0.0°$ to $-90.0°$, the guided modes in area III become progressively sharper. This appears to indicate that $\phi_1 = -90.0°$ is the best cell setting for the accurate measurement of the twist-off. However it is also clear from figure 3 (*a*) that the first mode in area III shifts to small internal angles as ϕ_1 moves from $-40.0°$ to $-90.0°$. This means that the sensitivity of the mode position to small changes of the twist-off may become lower, as illustrated in figure 4. For the first mode in the area III of figure 4 (*a*) the solid line is for a twist angle profile from $-90.0°$ to $-10.0°$, the dotted line is for $-90.5°$ to $-9.5°$ and the dashed line is for $-89.5°$ to $-10.5°$, while in figure 4 (*b*) the solid line is for $-55.0°$ to $25.0°$, the dotted line is for $-54.5°$ to $24.5°$ and the dashed line is for $-55.5°$ to $25.5°$. From these two figures it is clear that for the same changes of the twist-off situation, each surface changing by 0.5°, there is a 0.02° mode shift in figure 4 (*a*) and 0.06° in figure 4 (*b*). This means that there will be better resolution of the twist-off for the case of figure 4 (*b*). Furthermore in a real experiment, because of beam divergence of the radiation, we may not obtain such sharp modes as predicted in figure 4 (*a*). Bearing in mind the beam divergence and the internal angle limit from prism-coupling in a real

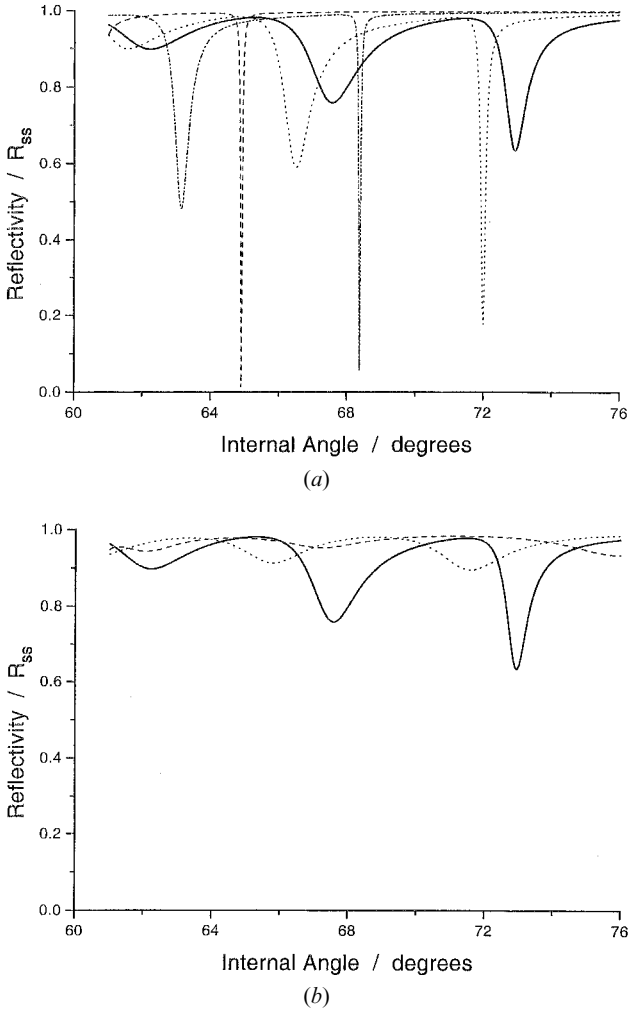

Figure 3. (*a*) Reflectivity data R_{ss} for four different twist-off situations; (*b*) reflectivity data R_{ss} for three different twist-off situations.

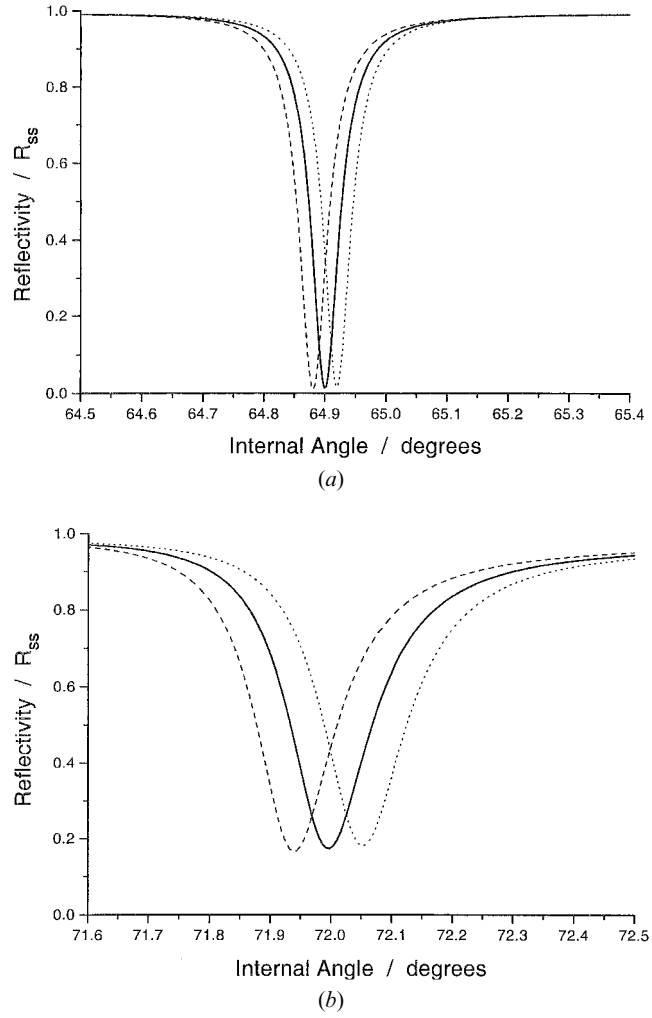

Figure 4. (*a*) R_{ss}, illustrating the shift of one guided mode for three different twist-off situations with ϕ_1 varying by $\pm 0.5°$ near to $-90.0°$. (*b*) R_{ss}, illustrating the shift of one guided mode for three different twist-off situations with ϕ_1 varying by $\pm 0.5°$ near to $-55.0°$.

experiment, the best window for accurate measurement of the twist-off of the TNLC cell will be for ϕ_1 on the top surface between $-50.0°$ and $-70.0°$.

3. Experimental

The sample geometry used is illustrated in figure 5. A high index ($n = 1.732$ at $\lambda = 632.8$ nm) glass plate and a low index ($n = 1.456$ at $\lambda = 632.8$ nm) glass substrate are spaced apart by 1.50 µm diameter glass-balls embedded in glue. Before assembly, both of the inner glass surfaces are coated with an aligning layer of polyimide film (PI32). The polyimide coating is prepared by first spin-coating an adhesion promoter which is baked at 100°C for about 1 min before cooling. Onto this is spin-coated a polyimide solution. The coated substrates are then baked for 4 h at 290°C before cooling and being uni-directionally rubbed using a velvet-covered drum. The cell is subsequently assembled with an angle of 86.0°

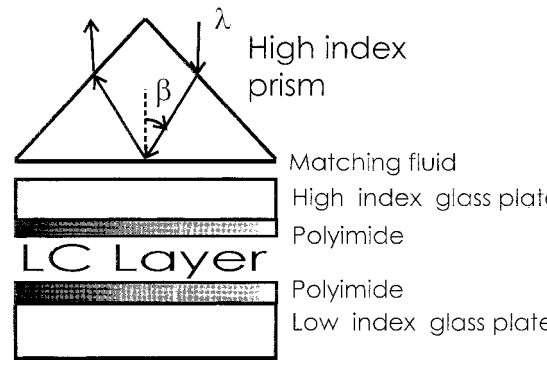

Figure 5. The experimental sample geometry.

between the two 'easy' axes on the inner surfaces, i.e. $\phi_t^0 = 86.0°$. Once assembled, the empty cell is placed in a temperature controlled environment having a stability

of 0.10°C, and heated to 75.0°C. At this temperature, the cell is capillary filled with the nematic liquid crystal E7 (Merck). When filled, the cell temperature is reduced at about 2.0°C h^{-1} to leave a monodomain at room temperature. This cooled cell is then optically matched to a high index ($n = 1.732$ at $\lambda = 632.8$ nm) prism by use of a suitable matching fluid (CH_2I_2) to give the complete experimental geometry shown in figure 5. The cell and prism are assembled so that the direction of the easy axis on the top surface is about $-60°$ away from the incidence plane to optimize the sample setting for accurate determination of the twist-off situation of the TN cell. Finally, in order to obtain the required angle-dependent reflectivity data as a function of the angle of incidence, the complete cell, in its temperature stabilized environment, is positioned on a computer controlled rotating table. Monochromatic, plane polarized, 632.8 nm radiation from a HeNe laser is arranged to arrive at the centre of the sample and appropriate sets of angle-dependent reflectivity data are then recorded as reported elsewhere [13, 14].

4. Results and discussion

Two typical data sets (crosses) for both R_{SS} and the p to s polarization conversion signal, R_{PS}, at room temperature (24.5°C) are shown in figures 6(*a*) and 6(*b*). To model the optics of this TN cell structure theoretically, a scattering matrix approach [15] is used. Combining this with a steepest decent minimization fitting routine gives the director profile through the cell. In order to reduce the search time and minimize degeneracy problems between surface layers and the NLC itself, a set of polarization conserving signals, R_{PP} and R_{SS}, have been recorded for another test cell which is fabricated by the same procedure and at the same time as the first one but which is filled with silicone oil instead of the NLC material. For this simple situation, with the primary part of the cell having only an isotropic index, fitting of the R_{PP} and R_{SS} data gives the parameters of the polyimide layers of the second test cell. Then we use these parameters as estimated values to start the fitting for the NLC cell. In addition, the variation of the optical permittivity of E7 (Merck) with temperature has been accurately measured in Exeter by the guided mode method in recent years and so these parameters can also be closely bounded to reduce any director profile degeneracy problem in the fitting. The final fits are given by the full curves in figures 6(*a*) and 6(*b*). For a reduced angle range, the experimentally recorded R_{SS} data (crosses) and its theoretical fit (solid curve) are shown in figure 7 to show the detail of the fitting of the first mode in figure 6(*a*) and to indicate the accuracy of the fitting. The parameters established for the TN cell by this fitting are: for the high index glass plate $\varepsilon_H = 2.9998$

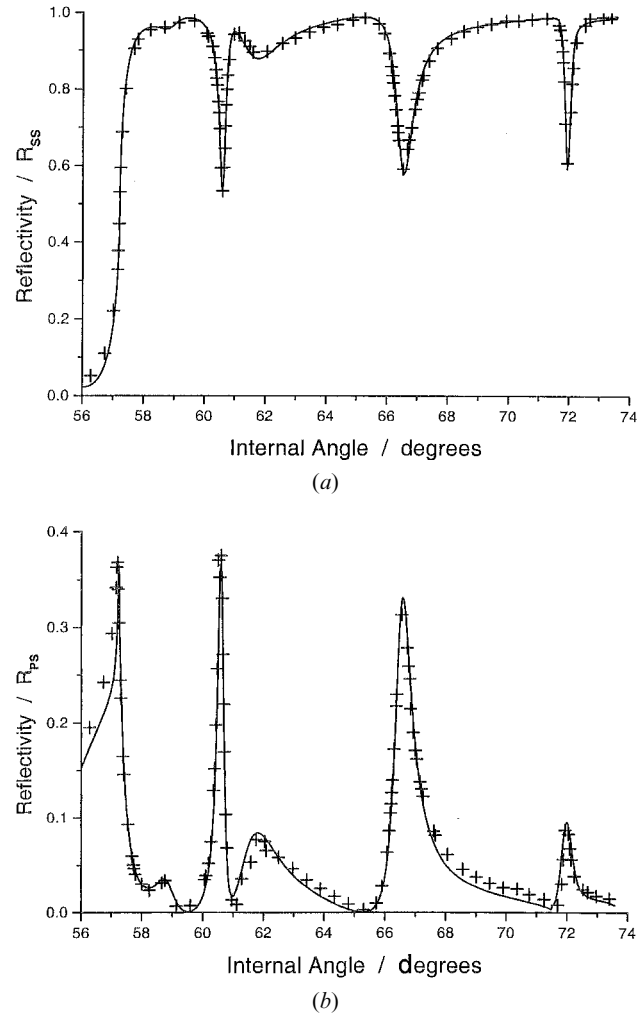

Figure 6. (*a*) Experimentally recorded R_{SS} (crosses) together with theoretical fitting (solid line); (*b*) experimentally recorded R_{PS} (crosses) together with theoretical fitting (solid line).

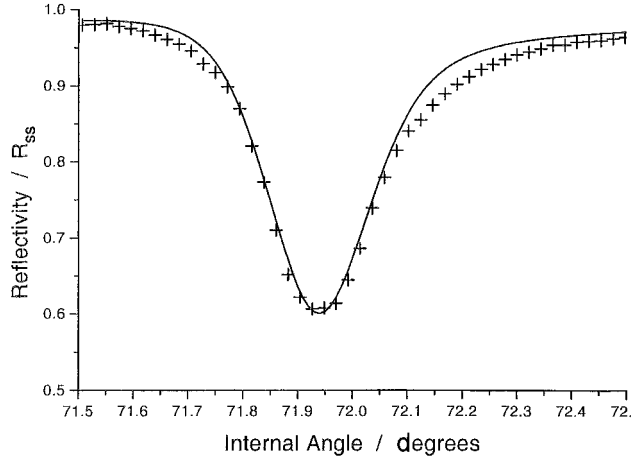

Figure 7. Details of the first mode in area III: experimental data for R_{SS} (crosses) and theoretical fitting (solid line).

($n_H = 1.7320$); for the low index glass plate $\varepsilon_L = 2.1207$ ($n_L = 1.456$); for the polyimide alignment layers $\varepsilon_P = 2.3434 + i0.0026$ and $d_P = 61.4$ nm and for the E7, $\varepsilon_{\parallel} = 2.9921 + i0.0002$, $\varepsilon_{\perp} = 2.3043 + i0.0004$ with $d_{LC} = 1.535$ μm. The twist angle varies linearly from $\phi_1 = -56.81°$ on the top surface to $\phi_2 = 18.02°$ on the bottom surface, while the tilt angle varies linearly from 92.0° at the top to 88.0° at the bottom, i.e. there is approximately a 2.0° pre-tilt angle on the polyimide alignment layers. The linear variation of tilt and twist angles may be predicted from continuum theory [16]. For no applied field the twist ϕ and tilt θ are specified by the following two equations:

$$(1 + \alpha \cos^2\theta) \sin^2\theta (d\phi/dz) = C_1 \tag{1}$$

and

$$(1 + \eta \cos^2\theta)(d\theta/dz)^2 + C_1^2(1 + \eta)/[(1 + \alpha)(1 + \alpha \cos^2\theta) \sin^2\theta] = C_2 \tag{2}$$

where

$$\alpha = (K_{33} - K_{22})/K_{22} \quad \text{and} \quad \eta = (K_{33} - K_{11})/K_{11} \tag{3}$$

and C_1 and C_2 are integration constants. From these equations it therefore appears that there is a complex relationship between the twist and tilt profiles in the cell. This will in general lead to other than linear twist and tilt profiles. However in the present case with $\theta_1 = 92°$, $\theta_2 = 88°$, $\phi_t = |\phi_1 - \phi_2| = 74.83°$, $d_{LC} = 1.535$ μm and using elastic constants for E7, we find after integration of these equations that the maximum predicted deviation of twist from linearity is $\sim 0.006°$, while for tilt, the maximum deviation is $\sim 0.02°$. These deviations from a simple linear variation across the cell are not experimentally distinguishable. In addition the experimental fitting indicates no variation from this linearity near either surface in our cell, suggesting that any order parameter variations close to the surfaces are, to the level of our experimental precision, not discernible.

As used above from the data fitting, we have $\phi_t = 74.83°$ and, with the knowledge of $\phi_t^0 = 86.0°$ from the cell fabrication, then $2\Delta\phi = |\phi_t^0 - \phi_t| = 11.17°$. According to the Rapini–Papoular [17] formulation, the anchoring free energy, $F_{Anchoring}$ is given by

$$F_{Anchoring} = -0.5 W_T \sin^2(\Delta\phi) \tag{4}$$

and the torque balances on the surfaces are:

$$K_{22}(d\phi/dz) = 0.5 W_T \sin(2\Delta\phi). \tag{5}$$

Hence we have

$$W_T = 2K_{22}\phi_t/[d_{LC} \sin(2\Delta\phi)]. \tag{6}$$

This gives $W_T = 5.79 \times 10^{-5}$ J m^{-2} using $d_{LC} = 1.535$ μm and $K_{22} = 6.6 \times 10^{-12}$ N [18]. The main uncertainty in the determination of W_T comes from $2\Delta\phi$. Because of the cell fabrication procedures the uncertainty of ϕ_t^0 is of the order 0.5°, while the uncertainty in determining ϕ_t from the fitting data is less than 0.2°. Therefore the total uncertainty of $2\Delta\phi$ is estimated to be less than about 0.7°, leading to a relative uncertainty in W_T of about 6%. Thus the final result for the surface torsional anchoring strength of E7 (Merck) on a rubbed polyimide alignment layer is $W_T = (5.8 \pm 0.4) \times 10^{-5}$ J m^{-2} at 24.5°C. This result is somewhat different from that previously reported [6] which gave $W_T = (2.9 \pm 0.2) \times 10^{-5}$ J m^{-2} on rubbed polyimide at 23.5°C. This difference will arise from different sample production, and in particular from different rubbing conditions.

It is important to point out that equation (4) is a special case of the more general form of surface anchoring:

$$F_{Anchoring} = -0.5 W(\mathbf{n}\ \mathbf{e})^2 \tag{7}$$

where $\mathbf{n} = (\sin\theta\cos\phi,\ \sin\theta\sin\phi,\ \cos\theta)$ and $\mathbf{e} = (\sin\theta_e\cos\phi_e, \sin\theta_e\sin\phi_e, \cos\theta_e)$. This may suggest that the surface twist anchoring equation (4) cannot be simply used as above. In order to show that equation (4) is satisfactory we need to develop the more general equation (7) using a variational approach. For a non-chiral system one of the two surface torque balance equations becomes [19]:

$$h(\theta)(d\phi/dz) = WB \sin\theta \sin\theta_e \sin(\phi - \phi_e) \tag{8}$$

where

$$h(\theta) = (K_{22} \sin^2\theta + K_{33} \cos^2\theta) \sin^2\theta \tag{9}$$

and

$$B = \sin\theta \sin\theta_e \cos(\phi - \phi_e) + \cos\theta \cos\theta_e. \tag{10}$$

From equations (8) to (10) we have

$$K_{22}(d\phi/dz) = 0.5 W \sin 2(\phi - \phi_e) C \tag{11}$$

where

$$C = \sin^2\theta_e/(1 + \alpha \cos^2\theta) + \cos\theta \cos\theta_e \sin\theta_e/\sin\theta \times (1 + \alpha \cos^2\theta) \cos(\phi - \phi_e). \tag{12}$$

It is clear that if $(\phi - \phi_e)$ is small and θ and θ_e are close to $\pi/2$, then C will be close to 1 and equation (11) will reduce to equation (5). For our case $(\phi - \phi_e) = 5.58°$ and $\theta \sim \theta_e \sim 92°$ (or $\sim 88°$). Substituting in such values with the known elastic constants gives $C = 0.998$. Thus we can safely use equation (5) and ignore the effect of pretilt angle on the surface director twist.

5. Conclusion

The HLGM technique has been used to excite a series of half-leaky guided modes in a thin TNLC cell. The

twisted alignment is realized by use of rubbed polyimide layers on the inner walls of the cell. Reflectivity data from the half-leaky guided modes is very sensitive to the director profile of the liquid crystal. By using multi-layer optics modelling to fit the reflectivity data of the half-leaky guided modes, the cell thickness and the twist of the director from the top to the bottom in the cell are accurately determined. Comparing the rubbing directions on the two surfaces with the twist of the easy axes, the torsional anchoring coefficient W_T is quantified through knowledge of the twist elastic constant K_{22} of E7. At 24.5°C we find for E7 on rubbed polyimide that $W_T = (5.8 \pm 0.4) \times 10^{-5}$ J m^{-2}.

The authors are grateful for the financial support of the Chinese Natural Science Foundation (CNSF-19874038) and the continuing support of the Engineering and Physical Sciences Research Council of the UK.

References

[1] Yokoyama, H., and van Sprang, H. A., 1985, *J. appl. Phys.*, **57,** 4520.
[2] Nastishin, Yu. A., Polak, R. D., Shiyanovskii, S. V., Bodnar, V. H., and Lavrentovich, O. D., 1999, *J. appl. Phys.*, **86,** 4199.
[3] Yang, F., and Sambles, J. R., 2000, *J. appl. Phys.*, **87,** 2726.
[4] Faetti, S., Nobili, M., and Schipone, A., 1991, *Liq. Cryst.*, **10,** 95.
[5] Faetti, S., and Nobili, M., 1998, *Liq. Cryst.*, **25,** 487.
[6] Hallam, B. T., Yang, F., and Sambles, J. R., 1999, *Liq. Cryst.*, **26,** 657.
[7] Yang, F., Sambles, J. R., and Bradberry, G. W., 1999, *J. appl. Phys.*, **85,** 728.
[8] Iimura, Y., Kobayashi, N., and Kobayashi, S., 1994, *Jpn. J. appl. Phys.*, **33,** L434.
[9] Jiang, M., Huang, X. M., Wang, Z. K., Ma, K., and Sun, R. P., 1995, *Liq. Cryst.*, **18,** 419.
[10] Polossat, E., and Dozov, I., 1996, *Mol. Cryst. liq. Cryst.*, **282,** 223.
[11] Akahane, T., Kaneko, H., and Kimura, M., 1996, *Jpn. J. appl. Phys.*, **35,** 4434.
[12] Yang, F., and Sambles, J. R., 1998, *Jpn. J. appl. Phys.*, **37,** 3998.
[13] Yang, F., and Sambles, J. R., 1993, *J. opt. Soc. Am.*, **B10,** 858.
[14] Yang, F., and Sambles, J. R., 1993, *Liq. Cryst.*, **13,** 1.
[15] Ko, D. Y. K., and Sambles, J. R., 1988, *J. opt. Soc. Am.*, **A5,** 1863.
[16] Deuling, H. J., 1974, *Mol. Cryst. liq. Cryst.*, **27,** 81.
[17] Rapini, A., and Papoular, M. J., 1969, *J. Phys. (Paris), Colloq.*, **30,** C4.
[18] Bancroft, M. J., 1991, PhD thesis, University of Manchester, UK.
[19] Sugimura, A., Luckhurst, G. R., and Ou-Yang, Z., 1995, *Phys. Rev. E*, **52,** 681.